sciendo

DOI: 10.2478/auoc-2022-0004

Ovidius University Annals of Chemistry Volume 33, Number 1, pp. 23 - 35, 2022

Molecular docking and pharmacokinetics studies of *Curcuma longa* (Curcumin) potency against Ebola virus

Adewusi John ADEPOJU,[1] Dayo Felix LATONA,[2] Oluwafemi Gbenga OLAFARE,[1] Abel Kolawole OYEBAMIJI,[3] Misbaudeen ABDUL-HAMMED,[1] and Banjo SEMIRE[*1]

[1]*Computational Chemistry Laboratory, Department of Pure and Applied Chemistry, Ladoke Akintola University of Technology, P.M.B. 4000, Ogbomoso, Oyo-State, Nigeria*
[2]*Department of Pure and Applied Chemistry, Osun State University, Osogbo, Nigeria*
[3]*Department of Basic Sciences, Adeleke University, P.M.B. 250, Ede, Osun State, Nigeria*

Abstract. The Ebola virus disease causing hemorrhagic fever in human, has been known for nearly about 40 years, with the most recent outbreak being in West Africa creating humanitarian crisis, where over 11,308 deaths were recorded as reported in 30th March, 2016 (World Health Organization). Till now, Ebola virus drugs have been far from achieving regulatory FDA approval, and coupled with toxicity of these drugs, it is become imperative to appraise the available trail drugs, as well as looking into alternative natural resources of tackling menace. Therefore, *in silico* methods were used to assess the potency of the bioactive phytochemical, Curcumin from Turmeric and results compared with those obtained for some selected trial drugs in use for the treatment of Ebola virus. This study is focused on molecular docking of Curcumin and eight commercially available drugs (Amodiaquine, Apilimod, Azithromycin, Bepridil, Pyronaridine, Remedesivir and Tilorone) against Ebola transcription activator **VP30** proteins (PDB: 2I8B, 4Z9P and 5T3T) and their ADMET profiling. The results showed that binding affinity (ΔG kJ/mol) ranged from -5.8 (Tilorone) to -7.3 (Remdesivir) for 218B, -6.4 (Tilorone) to -8.2 (Pyronaridine, Remedesivir) and -5.8 (Bepridil) to -7.4 (Pyronaridine). Curcumin could be more desirable as inhibitor for than Tilorone, Dronedarone and Bepridil in the treatment of Ebola virus; the ADMET profile revealed that Curcumin presents attractive pharmacokinetic properties than the trial drugs.

***Keywords*:** curcumin; docking; pharmacokinetics; Ebola virus.

1. Introduction

Ebola virus (EBOV) belongs to the Filovirus family and order Mononegavirales, it contains negative-sense single-stranded RNA with a protective envelope [1], which causes acute hemorrhagic fever with a high case-fatality rate in humans. According to WHO, five strains of EBOV have been identified, causing a total of 25 outbreaks and differentiated based on virulence properties and geographical patterns [2, 3] as follows: Zaire Ebola virus (ZEBOV), Bundibugyo Ebola virus (BDBV), Reston Ebola virus (RESTV), Sudan Ebola virus (SUDV), and Taï Forest Ebola virus (TAFV) strains named after the places affected by the outbreaks [4].

Recent outbreak in 2014 caused by the most lethal Zaire strain in West Africa affected Guinea, Liberia, and Sierra Leone, and Nigeria resulting in 11,000 deaths [5, 6]. The majority of transmission events were between family members (74%) caused by direct contact with the affected persons or bodies of those who died from External ventricular drains (EVD) through blood and contact with fluid body secretions. This has being the most dangerous and effective way of transmission of the virus [7]. The infection projects itself in two phases with symptoms ranging from fever, fatigue, rashes, vomiting in the early phase, whereas in the late phase hemorrhagic shock occurs eventually resulting in death [8].

However researchers have suspected the fruit bats as the most probable candidate species. Three different bat types are found to carry this virus without being affected that suggested them as a primary natural reservoir for Ebola viruses [9]. Infectious Ebola viruses have never been characterized from any fruit bat species except small amount of viral RNA fragments of Zaire Ebola virus around endemic areas [10]. The Ebola virus genomic RNA is consisted of around 19,000 nucleotides [11]. It encodes seven structural proteins, namely, nucleoprotein (NP), glycoprotein (GP), RNA-dependent RNA polymerase (L), matrix protein (VP40), and three nucleocapsid proteins (VP24, VP30, and VP35) [12-14].

In this work, computational methods were used to evaluate the inhibitory activity of Curcumin,that is major component of the extract of the medicinal plant Turmeric, via molecular docking and ADMET assessment. However, for effective discussion and robust evaluation, the results were compared with seven trial drugs (Amodiaquine, Apilimod, Azithromycin, Bepridil, Pyronaridine, Remedesivir, Dronedarone and Tilorone) commonly used for the treatment of patients with Ebola Virus. These drugs were docked against nucleoprotein (NP) of the Ebola virus; **2I8B, 4Z9P and 5T3T** [15-18], the transcription activator **VP30,** which is believed to play an essential role in Ebola virus replication, most likely by stabilizing nascent mRNA **2I8B** [16], nucleocapsid protein (NP) to facilitate

* Corresponding author. *E-mail address:* bsemire@lauctech.edu.ng (Banjo Semire)

genomic RNA encapsidation to form viral ribonucleoprotein complex (RNP) together with genome RNA and polymerase, which plays the most essential role in virus proliferation cycle, **4Z9P** [16]. The VP30 C-terminal domain interacts with a short peptide in the C-terminal region of NP which reveals that a conserved, proline-rich NP peptide binds a shallow hydrophobic cleft on the VP30 C-terminal domain **5T3T** [17]. The protein receptors were downloaded from the Protein Data Bank (PDB), a depository data bank that contains 3D structural information of large biological molecules such as proteins and nucleic acids (https://www.rcsb.org/structure). Also, the canonical SMILES for each ligand structure from the PubChem database (https://pubchem.ncbi.nlm.nih.gov) was copied and then taken to SymyxDraw to generate 2-D structure of the ligands, which is subsequently converted to 3-D structures.

2. Experimental

2.1. Molecular docking procedure

Prior to docking, the downloaded ligands were search for equilibrium conformers using semi-empirical AM1 method to find the conformer with lowest energy for each compound; this was then taken as starting structure for DFT calculations [18]. The equilibrium optimization and energy calculation were performed on the ligands with DFT of Becke's three parameter hybrid functional with correlation of Lee, Yang and Parr (B3LYP) [19] with 6-31G** basis set. Frequency calculations were examined to ascertain minima equilibrium as characterized by positive harmonic frequencies [20, 21] as implemented in Spartan 14 [22]. These optimized structures were taken for molecular Docking. The ligands were docked into the receptors by using Discovery studio, AutoDock Tools 1.5.6, AutoDock Vina 1.1.2 and Edu-PyMOL version 1.7.4.4. The receptors/proteins were cleaned up and repaired with Discovery Studio software and Edu-PyMOL was used to visualize the docking results. The binding pocket of the proteins were identified using 3DLigandSite -Ligand binding site prediction Server (https://www.wass-michaelislab.org/3dlig/) that is based on ligand-binding sites predictions using similar structures [23]. The binding pocket of the protein as observed in the crystal structure was set with the aid of AutoDock Tools, polar hydrogens were to the proteins, then Gasteiger charges was added before setting the grid box. The protein file was saved in pdbqt format and docking simulation was carried out using AutoDock Vina [24-32] for the calculation of binding affinity of the target receptor – ligand complex. Hydrogen bonding, and other hydrophobic interactions between the ligand and proteins were visualized using Discovery Studio 2019.

2.2. In-silico ADME/pharmacokinetic predictions

The optimized structure of the ligands were used for physicochemical and ADMET profiles of the ligands to assess the qualitative pharmacokinetics properties vis-a-vis; absorption, distribution, metabolism, excretion and toxicity by using ADMET Predictor 9.5 installation (www.simulations-plus.com). These have become imperative because information on physical properties as well as solvation properties relating to interactions of the ligand in different media and molecular characteristics are the intrinsic chemical reactivity of the ligand. These can be used to assess physical hazards, and to understand or predict a chemical's environmental fate and human toxicity.

3. Results and discussion

3.1. Docking conformation and binding affinity

Docking of transcription activator **VP30 [218B],** which is essential for Ebola virus replication with Amodiaquine, Apilimod, Azithromycin, Bepridil, Curcumin, Dronedarone, Pyronaridine, Remdesivir and Tilorone are presented in Table 1 and Figure 1. The binding energies for all the studied drugs with **2I8B** receptor are between -5.7 and -7.3 kcal/mol, this translated to inhibitory constant (Ki) of the drugs fall between 4.42 and 66.00 µM. This showed that Dronedarone has the least binding affinity of -5.7 kcal/mol, while Pyronaridine and Remdesivir are -7.2 and -7.3 kcal/mol, respectively (Table 1). The H-bond distances between amino acid residues in the binding purse and drug ranged from 2.0 to 3.3Å, and other forms of interactions between the ligand and the **218B** receptor are displayed in Figure 1. Amodiaquine showed hydrogen bond with TRP154 and THR'150; Apilimod LEU'247 and ARG'262; Azithromycin with LEU'247, ARG'262 and ARG'262; Curcumin with GLN'233, HIS'193, SER'234 and ASP'231; Pyronaridine with ASP'231 and ASP'231; Remdesivir with GLN'233, SER'234, ASP'231 and ASP'231. Pyronaridine displayed hydrophobic interactions with GLY'200, GLY'198, GLN'233, TRP'230, SER'234, GLN'203, LEU'199, VAL'207, PHE'238 and HIS'193; Remdesivir showed interactions with PHE'238, VAL'207, LEU'199, HIS'193, GLN'203, TRP'230, ASP'202, GLY'198 and GLY'200, whereas Curcumin displayed electrostatic interactions with **VAL'207, GLY'200, TRP'230, PHE'238, LEU'199, GLN'203** and **ASP'202.** The order of binding affinity in relation to the drug activeness against 2I8B are Remdesivir ≈ Pyronaridine > Apilimod > Amodiaquine > Bepridil > Azithromycin > Curcumin > Tilorone > Dronedarone. This in an indication that conformation of the ligand in the active gouge of the receptor (**2I8B**) pointed to Remdesivir and Pyronaridine as most active inhibitors against **2I8B;** thus Remdesivir and Pyronaridine could be said to be more potent than the active compound in Turmeric (Curcumin).

Table 1. Binding affinity and non-bonding interactions of **2I8B receptor** with the ligands+

Ligands	Binding affinity ΔG (kcal/mol)	Inhibition constant Ki (μM)	2I8B receptor amino acids forming H bond with ligands	H-bond distance (Å)	Electrostatic / Hydrophobic interactions involved
Amodiaquine	-6.5	17.09	TRP'154 THR'150	2.2 3.4	LEU170, LEU'173, ALA'169, THR'172, VAL'176, LEU'142, ILE'142
Apilimod	-6.7	12.19	LEU'247 ARG'262	2.1 2.0	LEU'144, ILE'148, CYS'251, VAL'265, LEU'261, VAL'258, GLU'252, PRO'250, GLN'248, LEU'249, ALA'246, PHE'181, GLN'185
Azithromycin	-6.2	28.36	LEU'247 ARG'262 ARG'262	3.3 2.3 2.6	GLU'152, GLN'248, VAL'258, GLU'252, LEU'261, VAL'265, CYS'251, LEU'144, PHE'181, ALA'246, ILE'148, LEU'247, LEU'249, PRO'250
Bepridil	-6.3	23.95			THR'146, THR'150, ILE'142, LEU'173, VAL'176, THR'172, LEU'147, ALA'169, LYS'166, LEU'170, TRP'154
Curcumin	-6.0	39.76	GLN'233 HIS'193 SER'234 ASP'231	2.1 2.2 2.5 2.8	VAL'207, GLY'200, TRP'230, PHE'238, LEU'199, GLN'203, ASP'202
Dronedarone	-5.7	66.00			SER'216, HIS'215, LEU'186, CYS'190, TYR'211, GLN'212, GLU'191, LEU'208, LEU'194, SER'184, SER'187, LEU'188, LYS'183
Pyronaridine	-7.2	5.24	ASP'231 ASP'231	3.3 3.1	GLY'200, GLY'198, GLN'233, TRP'230, SER'234, GLN'203, LEU'199, VAL'207, PHE'238, HIS'193
Remdesivir	-7.3	4.42	GLN'233 SER'234 ASP'231 ASP'231	2.4 2.2 3.2 2.9	PHE'238, VAL'207, LEU'199, HIS'193, GLN'203, TRP'230, ASP'202, GLY'198, GLY'200
Tilorone	-5.8	55.7			LYS'180, ARG'179, LEU'147, VAL'176, ILE'142, LEU'173, THR'150, ALA'169, TRP'154, LEU'170, LYS'166, THR'172

2D **3D**

Amodiaquine

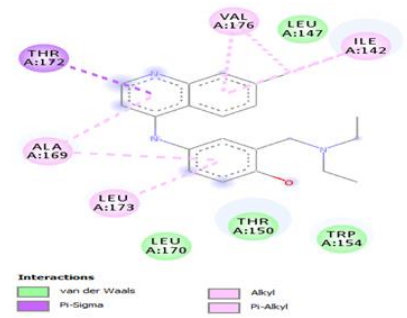

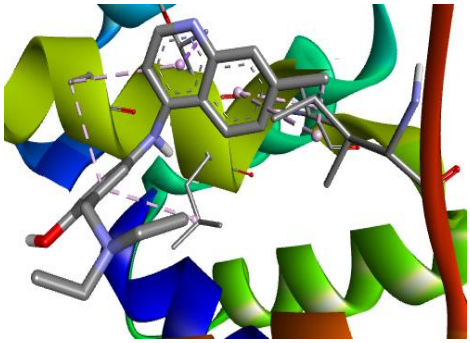

Apilimod

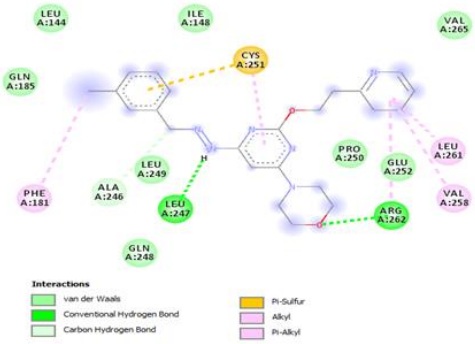

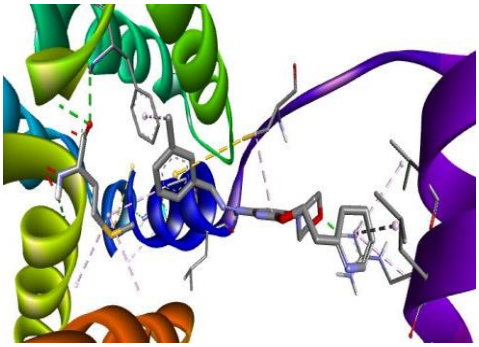

Azithromycin

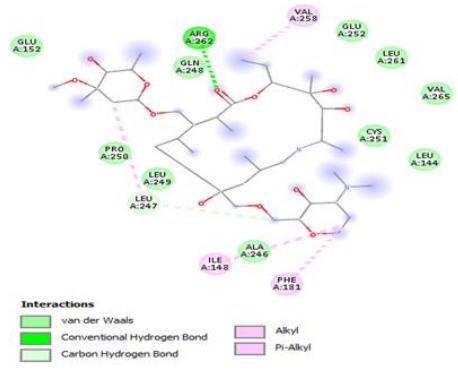

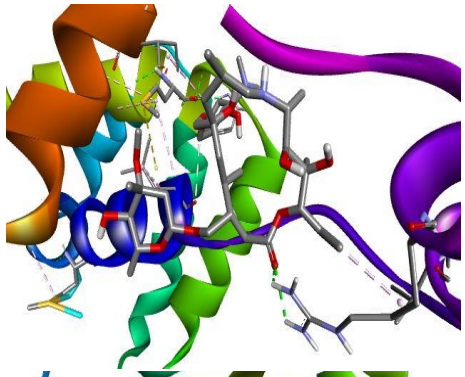

Bepridil

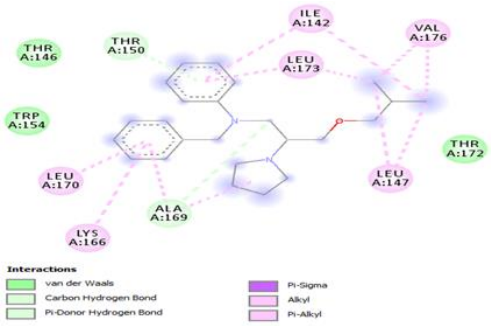

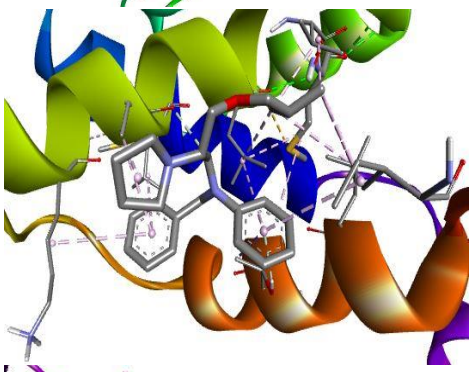

Dronedarone

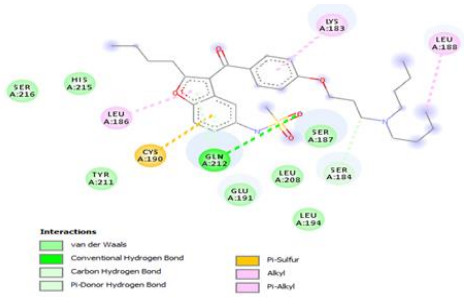

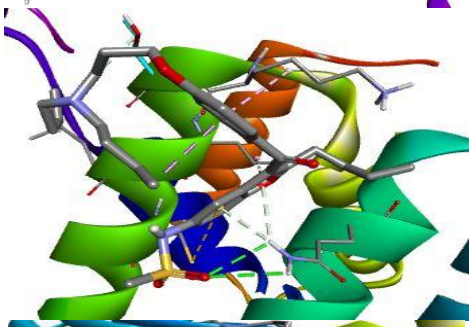

Pyronaridine

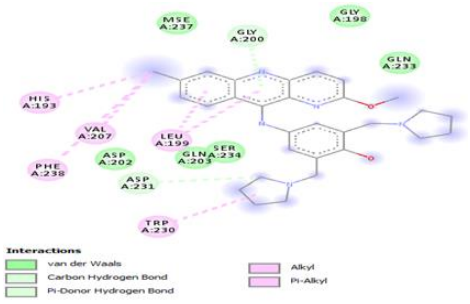

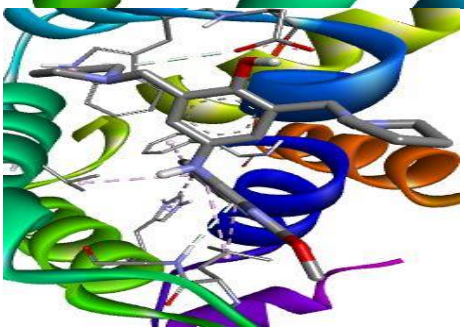

Remdesivir

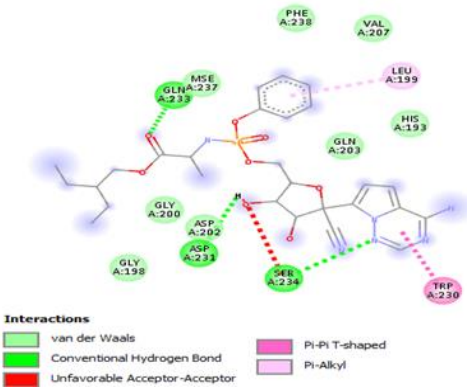

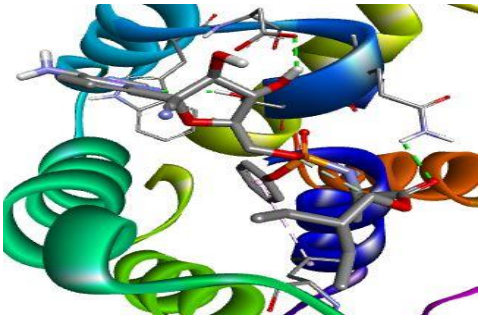

Tilorone

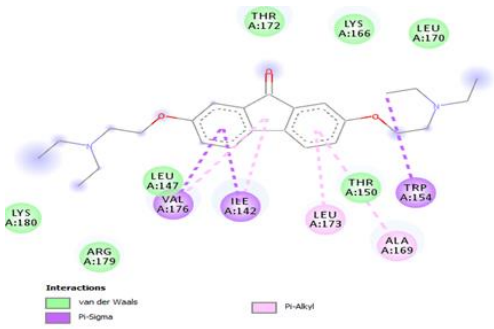

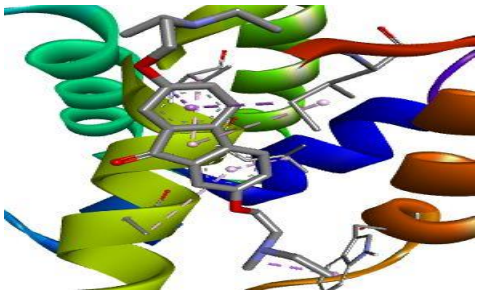

Curcumin

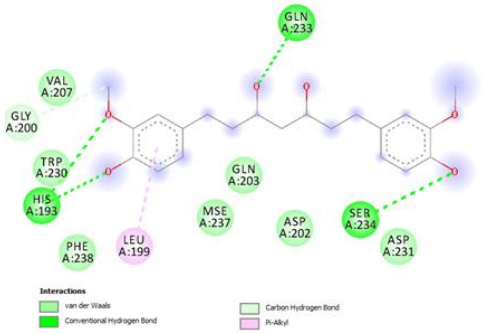

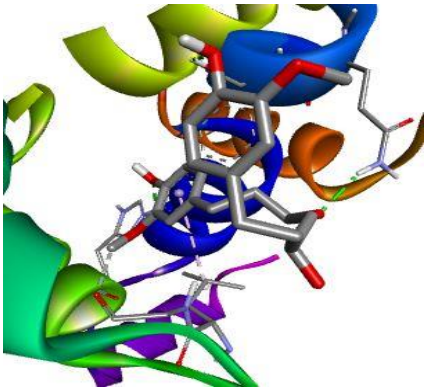

Figure 1. 2D and 3D of 218B interactions with the ligands

The calculated binding affinities for the ligands with **4Z9P** receptor showed that the drugs interacted with **4Z9P,** the nucleocapsid protein (NP) that facilitates genomic RNA encapsidation most essential to the Ebola virus proliferation than the **2I8B.** Tilorone has the binding affinity of -6.4 kcal/mol, Bepridil -6.7 kcal/mol, Curcumin -6.9 kcal/mol, Dronedarone -7.0 kcal/mol, Amodiaquine -7.1 kcal/mol, Apilimod -7.8 kcal/mol, Azithromycin -7.9 kcal/mol, Pyronaridine -8.2 kcal/mol and Remdesivir -8.2 kcal/mol (Table 2). The results were similar to the **4Z9P** receptor docked against using MOE 2014.09 software. The docking results revealed that Calbistrin C, α-Lipomycin, (R)-4-(ethylamino)-5-(2-hydroxy-5-((2S,4S,6S)-4-hydroxy-6-(4-hydroxy-3-methoxyphenethyl)tetrahydro-2H-pyran-2-yl)-3-methoxyphenoxy)pentanoic acid, Lappaol C, (2,3-dihydroamentoflavone 7,4′-dimethyl ether, Rhusflavone and Licochalcone A were
-7.92, -7.84, -7.49, -7.23, -7.24, -7.14 and -5.01 kcal/mol, respectively, with similar binding interactions [33]. Also, seventeen various traditional drug compounds were docked against 4Z9P. The results showed that four of these compounds; hesperidin, cucurbitacin, Ginsenoside RH_2, Ginsenoside RO and Calbistrin C had binding affinity score of -7.6, -7.6, -7.5, -7.4 and -6.4 kcal/mol, respectively. This showed that binding affinity of Curcumin against 4Z9P is comparable to other potential ligands of medicinal plants [34]. The H-bond formed between **4Z9P** receptor amino acid residues and the drugs are within 3.6Å, other hydrophobic interactions of the drugs with **4Z9P** are displayed in Figure 2. Tilorone is hydrogen bonded with GLN'67, GLY'63, VAL'199, ARG'202 and THR'206; Bepridil has H bond interaction with HIS'102, and hydrophobic interactions with ALA'35, HIS'290, LEU'302, LEU'300, TYR'98, ASN'301, PHE'208, ARG'39, PHE'104 and GLY'103; Curcumin is H-bonded with ARG'39, ARG'39, HIS'102, HIS'290 and ASN'301; Dronedarone ARG'39, ARG'39, THR'206 and GLY'103, and also has hydrophobic interactions with TYR'98, LEU'302, GLY'103, THR'206, LEU'300, PHE'104 and PHE'208. Also, Amodiaquine showed H-bond interaction with VAL'64 and GLN'67, hydrophobic interactions with GLU'68, ASN'207, ALA'70, ASP'65, THR'206, ARG'202, VAL'199, GLY'63 PHE'60, PHE'66 and LEU'203; Apilimod showed hydrophobic interactions with GLN'38, ALA'35, ARG'37, LEU'302, HIS'290, HIS'102, TYR'98, LEU'99, PHE'208, ASN'301, PHE'212, LEU'300 and PHE'104; Azithromycin ARG'39, ARG'39, ARG'39, GLU'68, THR'206 and THR'206; Pyronaridine showed hydrophobic interactions with PHE'201, ARG'205, ALA'70, ILE'200, PHE'60, VAL'64, PHE'66, GLY'63, LEU'203, ASP'65 and GLN'67, whereas Remdesivir is H-bonded to LEU'209, PHE'104, ARG'39, PHE'208, GLU'68, ALA'70, ASP'65, ARG'202, VAL'199, GLY'63, VAL'64, PHE'60, LEU'203 and ASP'71, and hydrophobically interacted with ASN'207, GLN'67, THR'206, GLN'67, ASP'65, GLN'67 and PHE'66 residues. Despite general increase in binding affinities of the drugs towards **4Z9P**, Pyronaridine, Remdesivir, Azithromycin and Apilimod could be active inhibitors for **4Z9P** more active than the active compound in Turmeric.

Table 2. Binding affinity and non-bonding interactions of **4Z9P** receptor with the ligands

Ligands	Binding Affinity ΔG (kcal/mol)	Inhibition constant Ki (μM)	4z9p receptor amino acids forming H bond with ligands	H-bond distance (Å)	Electrostatic / Hydrophobic interactions involved
Amodiaquine	-7.1	6.21	VAL'64 GLN'67	2.9 3.6	GLU'68, ASN'207, ALA'70, ASP'65, THR'206, ARG'202, VAL'199, GLY'63 PHE'60, PHE'66, LEU'203
Apilimod	-7.8	1.90	ARG'39 ARG'39	2.0, 2.4 2.3	GLN'38, ALA'35, ARG'37, LEU'302, HIS'290, HIS'102, TYR'98, LEU'99, PHE'208, ASN'301, PHE'212, LEU'300, PHE'104
Azithromycin	-7.9	1.60	ARG'39 ARG'39 ARG'39 GLU'68 THR'206 THR'206	2.4 2.7 2.5 3.0, 3.5 2.6 2.4	ALA'70, GLN'67, ASN'207, LEU'203, ARG'202, PHE'60, GLY'63, ASP'71, PHE'208, LEU'209, PHE'104, ASN'301, PHE'66, ASP'65, VAL'64
Bepridil	-6.7	12.19	HIS'102	3.6	ALA'35, HIS'290, LEU'302, LEU'300, TYR'98, ASN'301, PHE'208, ARG'39, PHE'104, GLY'103
Curcumin	-6.9	8.69	ARG'39 ARG'39 HIS'102 HIS'290 ASN'301	2.4 2.4 3.3 2.2 2.1	TYR'98, LEU'302, GLY'103, THR'206, LEU'300, PHE'104, PHE'208
Dronedarone	-7.0	7.34	ARG'39 ARG'39 THR'206 GLY'103	2.5 2.5 3.3 2.1	GLN'38, ARG'37, ALA'35, SER'303, HIS'102, LEU'302, HIS'290, TYR'98, PHE'104, ASN'301, ILE'41, ASP'71, ASN'207, ASN'67, GLU'68, ALA'70 LEU'300, PHE'208
Pyronaridine	-8.2	0.96	VAL'199 ARG'202 ARG'202 THR'206	3.4 2.1 2.5 2.1	PHE'201, ARG'205, ALA'70, ILE'200, PHE'60, VAL'64, PHE'66, GLY'63, LEU'203, ASP'65, GLN'67
Remdesivir	-8.2	0.96	ASN'207 GLN'67 THR'206 GLN'67 ASP'65 GLN'67 PHE'66	2.5, 2.6 3.3 2.2 2.7 2.8, 2.9 2.5 2.8	LEU'209, PHE'104, ARG'39, PHE'208, GLU'68, ALA'70, ASP'65, ARG'202, VAL'199, GLY'63, VAL'64, PHE'60, LEU'203, ASP'71
Tilorone	-6.4	20.23	GLN'67 GLY'63 VAL'199 ARG'202 THR'206	3.3 3.4 3.2 3.4 2.0	GLU'68, ASP'71, ASN'207, ALA'70, PHE'66, ASP'65, LEU'203, VAL '64

Amodiaquine

2D

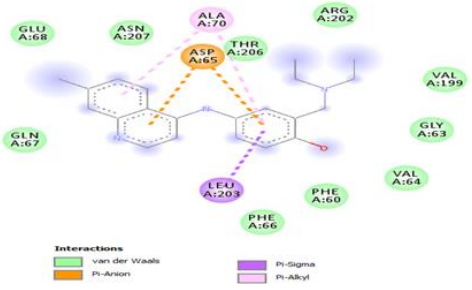

3D

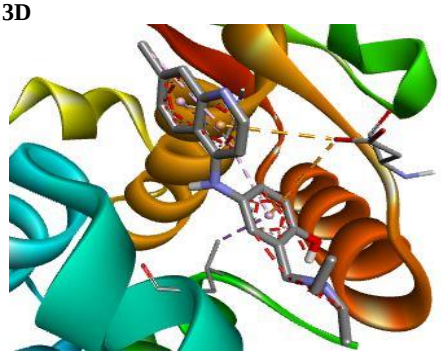

Apilimod

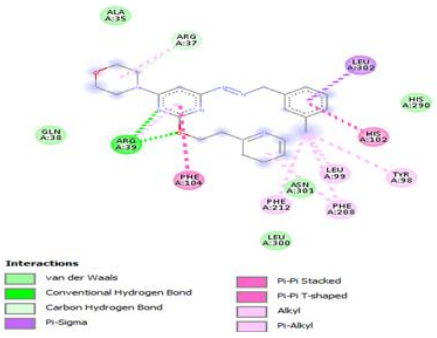

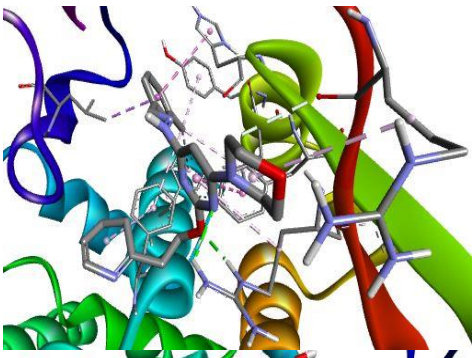

Azithromycin

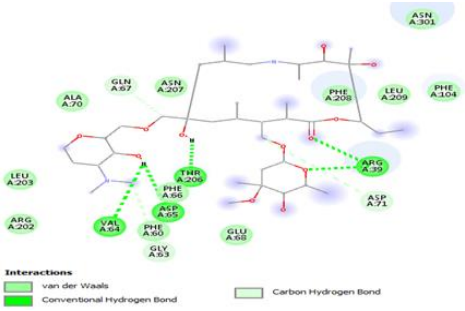

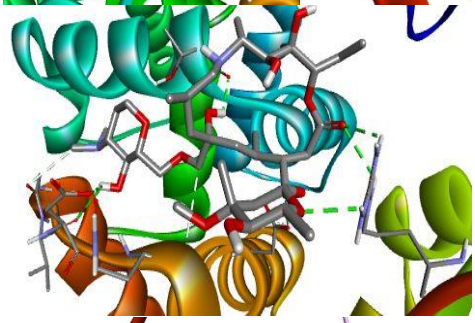

Bepridil

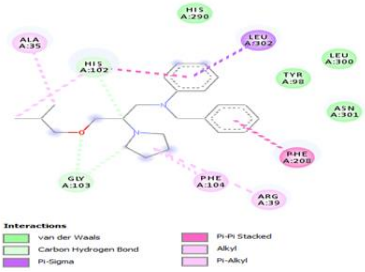

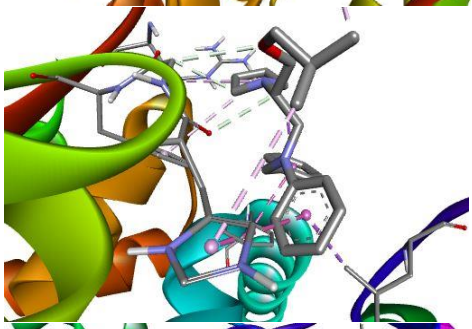

Dronedarone

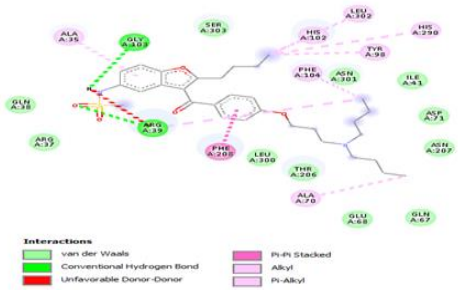

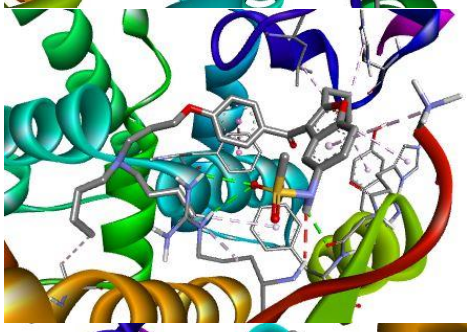

Pyronaridine

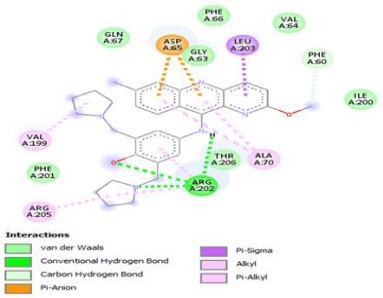

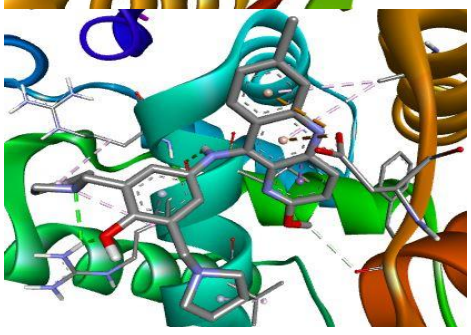

Remdesivir

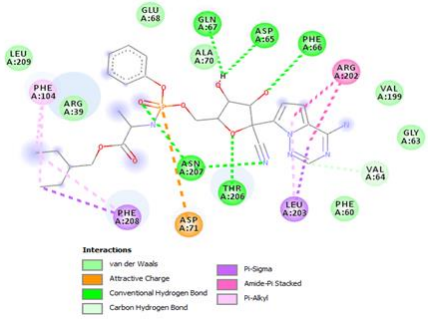

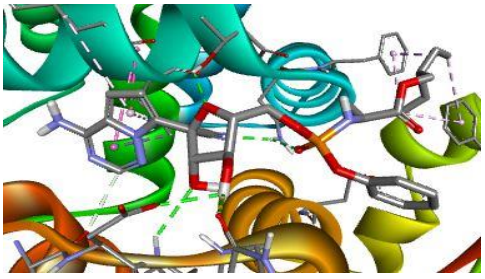

Tilorone

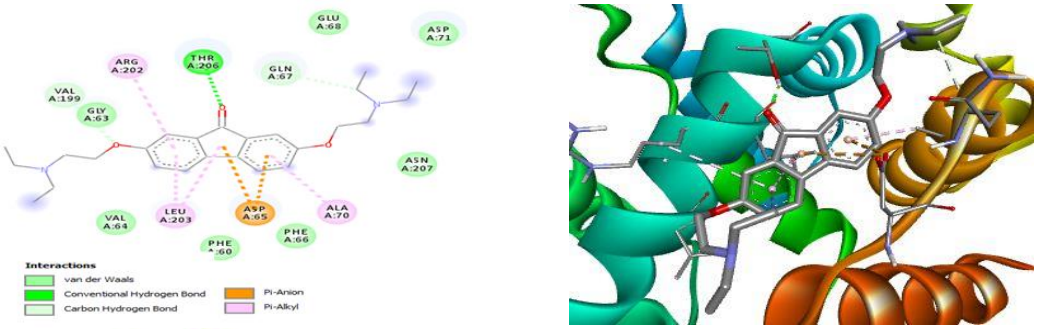

Curcumin

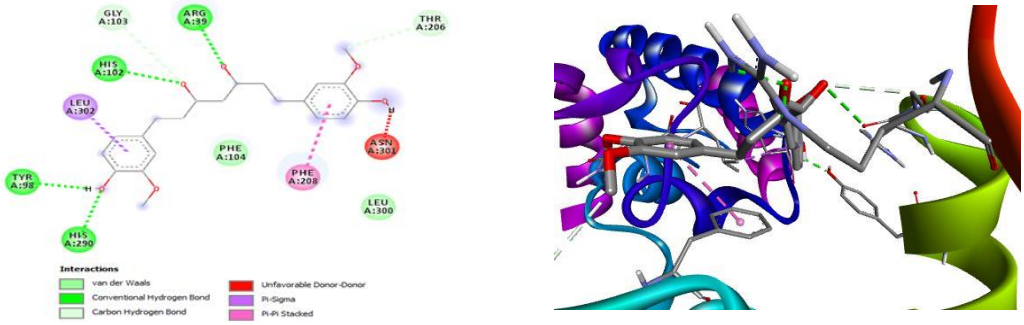

Figure 2. 2D and 3D interactions of **4Z9P** with the ligands

Likewise**,** results of docking simulations for the investigated ligands with **5T3T** receptor showed that Bepridil and Dronedarone have the binding affinity of -5.8 kcal/mol, Curcumin -6.6 kcal/mol, Amodiaquine and Azithromycin has -6.8 kcal/mol, Remdesivir and Tilorone has -7.0 kcal/mol Apilimod and Pyronaridine -7.4 kcal/mol and. The H-bond distances between amino acid residues in the binding purse and drug are with the 3.3Å radius (Table 3 and Figure 3). Curcumin showed H-bond interactions with GLU'197, SER'234, GLU'209 and ARG'213, and also interacted hydrophobically with GLN'229, LEU'226, PHE'222, VAL'210, TRP'230, PRO'206, PHE'238, HIS'193, LEU'199, MET'237 and HIS'193; Azithromycin interacted by hydrogen bonding with SER'234 and TRP'230. Amodiaquine shows hydrophobic interactions with VAL'207, PRO'206, PHE'238, LEU'199, HIS'193, MET'237, SER'234, GLN'233 and TRP'230, Apilimod interacted with ASP'231, TRP'230, PHE'222, ARG'213, GLU'209, VAL'210, PRO'206, PHE'238, HIS'193, ALA'241, GLU'197, MET'237 and LEU'199. Bepridil is Hydrophobic interacted with LEU'199, PRO'206, HIS'193, MET'237, GLU'197, PHE'238, VAL'207, GLN'203, TRP'230, and ASP'231; Dronedarone with GLN'203, PRO'206, GLU'209, VAL'210, PHE'222, VAL'207, LEU'199, MET'237 GLU'197, HIS'193, PHE'238, SER'234 and TRP'230. Pyronaridine is H-bonded to SER'234 and GLU209; and Remdesvir to TRP'230, ARG'213, GLU'209 and GLU'209. The NP-binding site on **5T3T** has been reported to be mostly hydrophobic interactions [35].

The order of binding affinity of the ligands against **5T3T** are Apilimod > Pyronaridine > Remdesivir > Tilorone > Azithromycin > Amodiaquine > Curcumin > Dronedarone > Bepridil. This showed that Apilimod, Pyronaridine, Remdesivir and Tilorone are more active inhibitors against **5T3T.**

Table 3. Binding affinity and non-bonding interactions of **5T3T** with the ligands

Ligands	**Binding Affinity ΔG (kcal/mol)**	**Inhibition constant K1 (μM)**	**5t3t receptor amino acids forming H bond with ligands**	**H-bond distance (Å)**	**Electrostatic / Hydrophobic interactions involved**
Amodiaquine	-6.8	10.30	GLU'197	2.9	VAL'207, PRO'206, PHE'238, LEU'199, HIS'193, MET'237, SER'234, GLN'233, TRP'230
Apilimod	-7.4	3.74	SER'234	2.3	ASP'231, TRP'230, PHE'222, ARG'213, GLU'209, VAL'210, PRO'206, PHE'238, HIS'193, ALA'241, GLU'197, MET'237, LEU'199
Azithromycin	-6.8	10.30	SER'234 TRP'230	2.5, 2.5 2.2	GLN'203, LEU'226, GLNV229, ARG'213, GLU'209, PHE'222, MET'237, VAL'210, LEU'199, HIS'193, PHE'238, VAL'207, ASP'231
Bepridil	-5.8	55.74	SER'234	3.3	LEU'199, PRO'206, HIS'193, MET'237, GLU'197, PHE'238, VAL'207, GLN'203, TRP'230, ASP'231

Ligands	Binding Affinity ΔG (kcal/mol)	Inhibition constant K1 (μM)	5t3t receptor amino acids forming H bond with ligands	H-bond distance (Å)	Electrostatic / Hydrophobic interactions involved
Curcumin	-6.6	14.43	GLU'197 SER'234 GLU'209 ARG'213	2.6 2.6 3.0 2.7	GLN'229, LEU'226, PHE'222, VAL'210, TRP'230, PRO'206, PHE'238, HIS'193, LEU'199, MET'237, HIS'193
Dronedarone	-5.8	55.74			GLN'203, PRO'206, GLU'209, VAL'210, PHE'222, VAL'207, LEU'199, MET'237 GLU'197, HIS'193, PHE'238, SER'234, TRP'230
Pyronaridine	7.4	3.74	SER'234 GLU209	2.6 3.1	ASP'231, VAL'210, LEU'226, PHE'222, ARG'213, PRO'206, GLU'205, VAL'207, LEU'199, HIS'193, PHE'238,TRP'230
Remdesivir	-7.0	7.35	TRP'230 ARG'213 GLU'209 GLU'209	2.2 2.6 3.1 3.2	MET'237, LEU'199, PHE'238, HIS'193, VAL'207, GLN'203, SER'234, ASP'231, LEU'226, ALA'225, GLN'229, PHE'222, VAL'210, PRO'206
Tilorone	-7.0	7.35	HIS'193	2.0	MET'237, LEU'199, GLU'197, PHE'238, VAL'207, TRP'230, VAL'210, PRO'206, GLU'209, LEU'226, PHE'222

2D **3D**

Amodiaquine

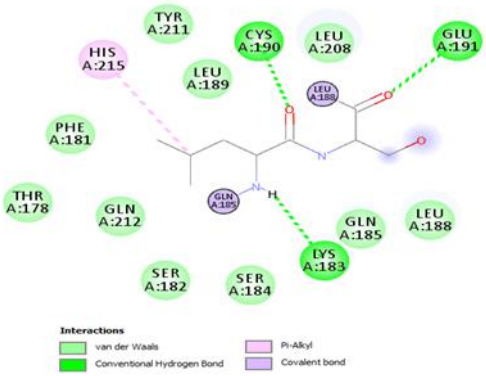

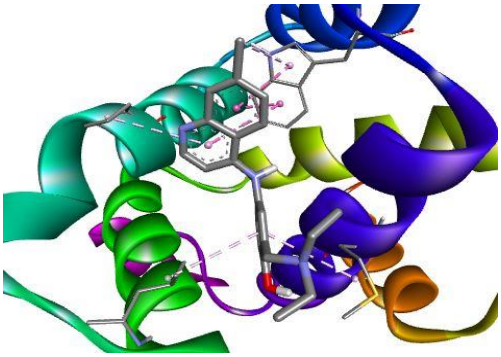

Apilimod

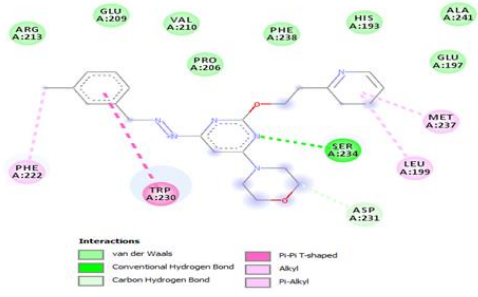

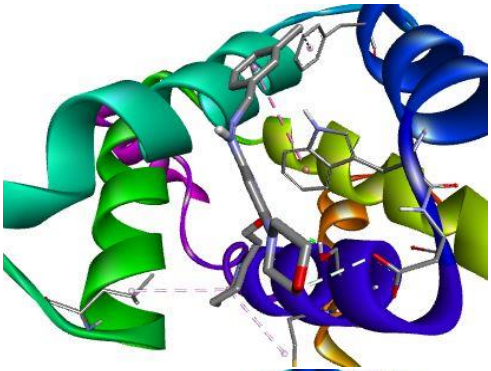

Azithromycin

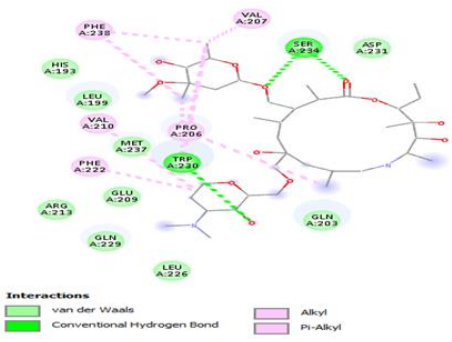

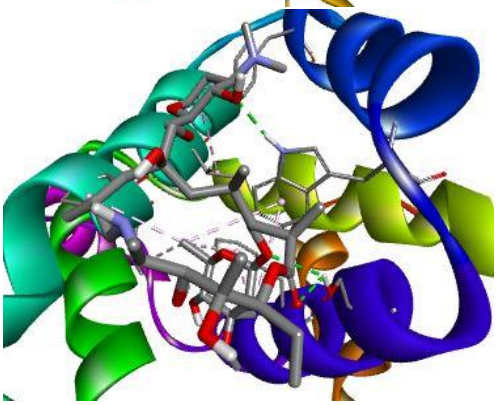

Bepridil

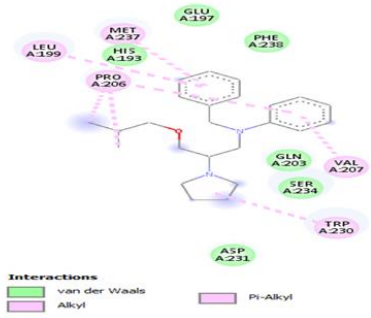

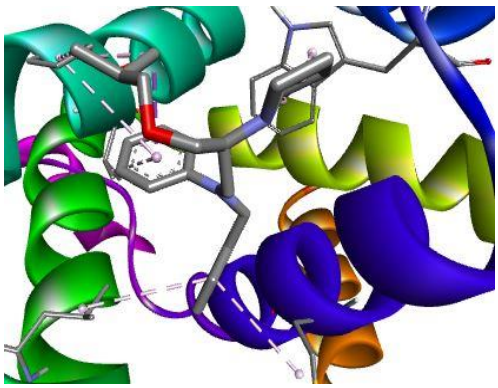

Dronedarone

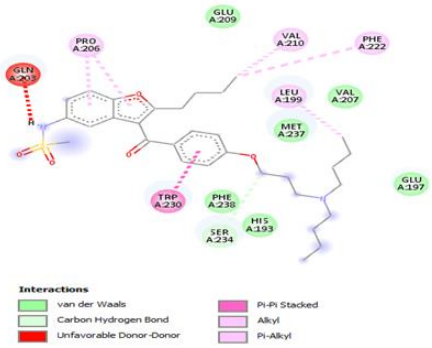

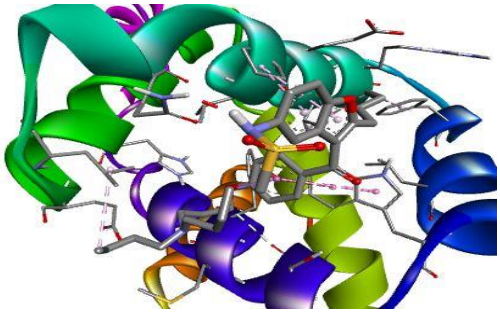

Favipiravir

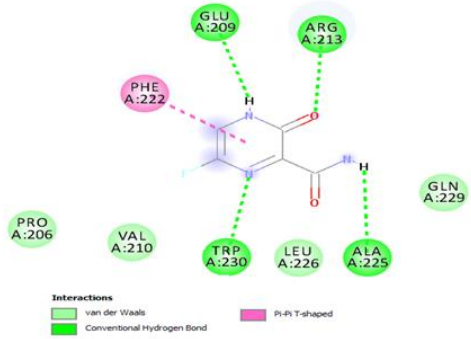

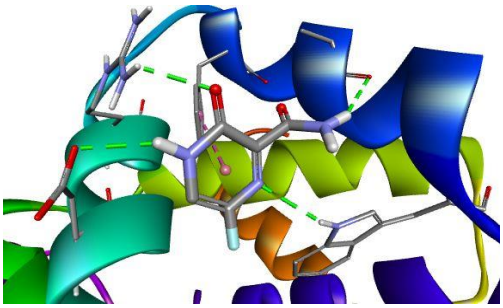

Pyronaridine

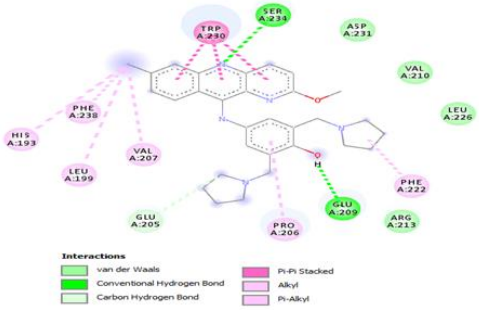

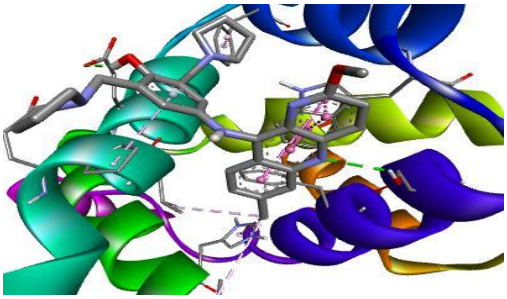

Remdesivir

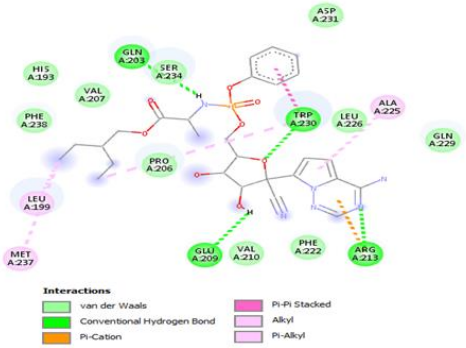

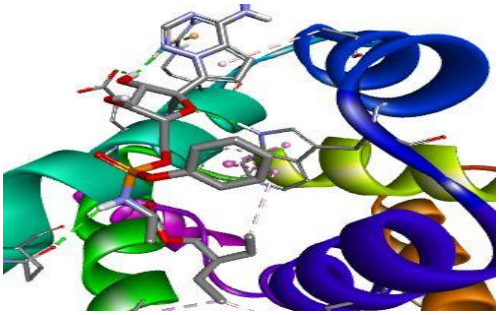

Tilorone

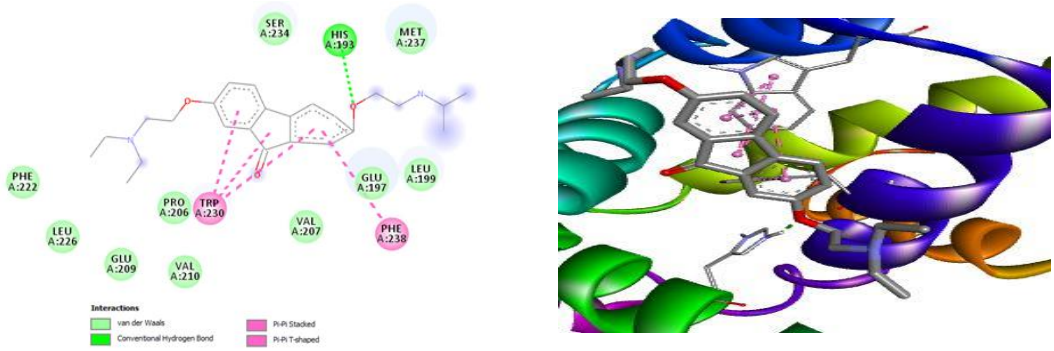

Curcumin

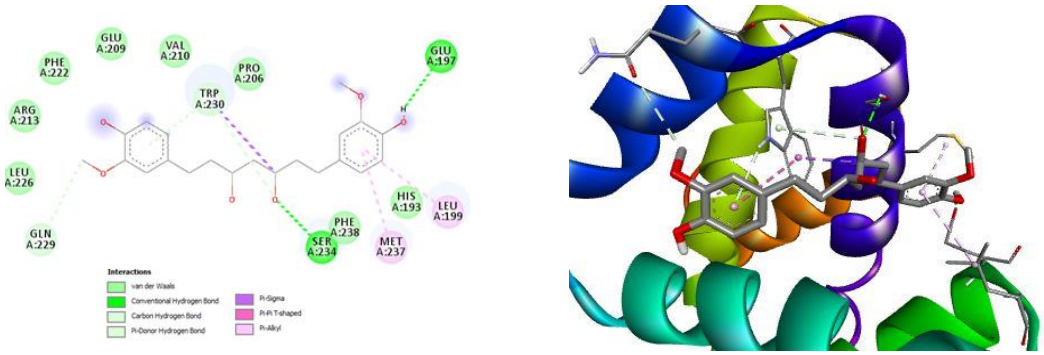

Figure 3. 2D and 3D interactions of **5T3T** with the ligands

3.2. ADME/pharmacokinetic predictions

In medicinal plants and drugs usage, safety is highly important; in this paper, the physiochemical properties of the ligands were assessed via ADMET profile. Drugs or active plant phytochemicals used for the therapeutical treatment should pass required physiochemical properties such as solubility, failure of ligands drug-ability have been linked to poor pharmacokinetics, solubility and bioavailability [36]. Hence, use of ADMET profiling is considered as one way to reduce inconvenient challenges associated with clinical trial treatments [37]. The Lipinski's rule of five [38] and ADMET properties predictors [39-41] were used to this evaluation. All the ligands passed the Lipinski's rule except Remdesivir and Azithromycin, also the bioavailability score of these two ligands showed were very low (Table 4). Apilimod, Pyronaridine, Tilorone, Amodiaquine, Curcumin and Bepridil have high GI absorption, and Tilorene, Bepridil and Amodiaquine possess blood–brain barrier BBB penetration. Pyronaridine, Remdesivir, Azithromycin Dronedarone and Bepridil were identified as P-gp substrate (i.e. they can be transported out of the cell). Cytochrome P450 isoforms inhibition may induce to drug-drug interactions which causes drugs metabolism failure when co-administered, in that way it lead to increase in toxic accumulation in the body [42], some of the ligands seemed to be P450 isoforms none inhibitors, it has been reported that inhibition of this protein could increase a compound in the plasma and decrease the clearance of its substrate [43]. However, Amodiaquine, Apilimod and Pyronaridine could be inhibitors to CYP2C19, Amodiaquine, Pyronaridine and Dronedarone could be inhibitors, CYP 2C9 could be inhibited by Apilimod, Pyronaridine and Curcumin; and Azithromycin could be none inhibitor to CYP 2D6 and CYP 3A4 (Table 5).

Table 4. Drug likeness of the ligands

Drugs	Lipinski	Ghose	Veber	Egan	Muegge	Bioavailability score
Amodiaquine	Yes	Yes	Yes	Yes	No	2.60
Apilimod	Yes	Yes	Yes	Yes	Yes	0.55
Azithromycin	No	No	No	No	No	0.17
Bepridil	Yes	Yes	Yes	Yes	No	0.55
Dronedarone	Yes	No	No	No	No	0.55
Pyronaridine	Yes	No	Yes	Yes	Yes	0.55
Remdesivir	No	No	No	No	No	0.17
Tilorone	Yes	Yes	No	Yes	Yes	0.55
Curcumin	Yes	Yes	Yes	Yes	Yes	0.55

Table 5. Pharmacokinetics

Drugs	GI Absorption	BBB Permeant	p-gp Substrate	CYP1A2 Inhibitor	CYP2C19 Inhibitor	CYP2C9 Inhibitor	CYP2D6 Inhibitor	CYP3A4 Inhibitor	Log K_p (skin permeation) cm/s
Amodiaquine	High	Yes	No	Yes	Yes	No	Yes	Yes	-4.79
Apilimod	High	No	No	No	Yes	Yes	Yes	Yes	-6.13
Azithromycin	Low	No	Yes	No	No	No	No	No	-8.01

Drugs	GI Absorption	BBB Permeant	p-gp Substrate	CYP1A2 Inhibitor	CYP2C19 Inhibitor	CYP2C9 Inhibitor	CYP2D6 Inhibitor	CYP3A4 Inhibitor	Log K_p (skin permeation) cm/s
Bepridil	High	Yes	Yes	No	No	No	Yes	Yes	-4.77
Dronedarone	Low	No	Yes	Yes	No	Yes	Yes	Yes	-4.56
Remdesivir	Low	No	Yes	No	No	No	No	Yes	-8.62
Pyronaridine	High	No	Yes	Yes	Yes	No	Yes	No	-5.95
Tilorone	High	Yes	No	No	No	No	Yes	Yes	-5.49
Curcumin	High	No	No	No	No	Yes	No	Yes	-6.28

4. Conclusion

This study emphasized assessment of curcumin, an active compound of Turmeric, a medicinal plant and eight popular trial drugs against different target proteins of Ebola virus by hindering the replication event in transcription activator **VP30** of the virus life cycle and/or by inhibiting of viral RNA synthesis RNA essential for virus proliferation cycle via Molecular Docking and ADMET prediction. The results showed that Remdesivir and Pyronaridine could be more active as inhibitors against **2I8B;** Pyronaridine, Remdesivir, Azithromycin and Apilimod could be more potent as inhibitors against **4Z9P**; and Apilimod, Pyronaridine, and Remdesivir could be more potent as inhibitors against **5T3T.** In general**,** the active compound in Turmeric (Curcumin) could be more desirable as inhibitor for than Tilorone, Dronedarone and Bepridil in treatment of Ebola virus. Also, this study also shown that all the inhibitors have more affinity for nucleocapsid protein (NP) that facilitates genomic RNA encapsidation. The ADMET properties showed that Curcumin has attractive pharmacokinetic properties than other inhibitors/ligands on trial.

Conflict of interest

The authors declare that there exist no financial or any conflict of interest whatsoever among them.

References

[1]. T.W. Geisbert, P.B. Jahrling, Differentiation of filoviruses by electron microscopy, Virus Research 39 (1995) 129-150.

[2]. E. Picazo, F. Giordanetto, Small molecule inhibitors of Ebola virus infection, Drug Discovery Today 20 (2015) 277–286.

[3]. World Health Organization (WHO). Ebola Situation Report March 30 (2016). https://www.who.int/csr/disease/ebola/en/

[4]. J.J. Suschak, C.S. Schmaljohn Vaccines against Ebola virus and Marburg virus: recent advances and promising candidates human, Vaccines and Immunotherapeutics 15 (2019) 2359-2377.

[5]. S.A. Moghadam, Z. Abdollahi, S.R. Fakour, A. A. Moghaddam, F. Kiany, N. Damani, The Relationship Between Periodontal Disease and Public Health: A Population-Based Study, Global Journal of Health Science 8 (2015) 110-115. DOI: 10.5539/gjhs.v8n7p110

[6]. S. Baize, D. Pannetier, L. Oestereich, T. Rieger, L. Koivogui, N. Magassouba, B. Soropogui, M. S. Sow, S. Keïta,, H. De Clerck, A. Tiffany, G. Dominguez, M. Loua, A. Traoré, M. Kolié, E. R. Malano, E. Heleze,, A. Bocquin, S. Mély, H. Raoul, V. Caro, D. Cadar, M. Gabriel, M. Pahlmann, D. Tappe, J. Schmidt-Chanasit, B. Impouma, A. K. Diallo, P. Formenty, M. V. Herp, S. Günther, Emergence of Zaire Ebola virus disease in Guinea, New England Journal of Medivine 371 (2014) 1418-1425. DOI: 10.1056/NEJMoa1404505

[7]. R.K Singh, K. Dhama, Y.S. Malik, M. Andavar Ramakrishnan, K. Karthik, R. Khandia, R. Tiwari, A. Munjal, M. Saminathan, S. Sachan, P.A. Desingu, J.J. Kattoor, H.M.N. Iqbal, S.K. Joshi. Ebola virus – epidemiology, diagnosis, and control: threat to humans, lessons learnt, and preparedness plans – an update on its 40 year's journey, Veterinary Quarterly 37 (2017) 98-135.

[8]. F. Chiappelli, A. Bakhordarian, A.D. Thames, A.M. Du, A.L. Jan, M. Nahcivan, M.T. Nguyen, N. Sama, E. Manfrini, F. Piva, R.M. Rocha, C.A. Maida, Ebola: translational science considerations, Journal of Translational Medicine 13 (2015) 11-15.

[9]. N.J. Beeching, M. Fenech, C.F. Houlihan, Critical Review: Ebola virus disease, British Medical Journal 349 (2014) g7348. DOI: 10.1136/bmj.g7348

[10]. H. Ogawa, H. Miyamoto, E. Nakayama, R. Yoshida, I. Nakamura, H. Sawa, A. Ishii, Y. Thomas, E. Nakagawa, K. Matsuno, M. Kajihara, J. Maruyama, N. Nao, M. Muramatsu, M. Kuroda, E. Simulundu, K. Changula, B. Hang'ombe, B. Namangala, A. Nambota J. Katampi, M. Igarashi, K. Ito, H. Feldmann, C. Sugimoto, L. Moonga, A. Mweene, A. Takada, Seroepidemiological prevalence of multiple species of filoviruses in fruit bats (*Eidolon helvum*) migrating in Africa, Journal of Infectious Diseases 212 (2015) S101-S108.

[11]. T. Ikegami, Molecular biology and genetic diversity of Rift Valley fever virus, Antiviral Research 95 (2012) 293-310.

[12]. O. Oluwagbemi, O. Awe, A comparative computational genomics of Ebola virus disease strains: Insilico insight for Ebola control, Informatics in Medicine Unlocked 12 (2018) 106–119.

[13]. M. Balmith, E.S. Soliman, Potential Ebola drug targets – filling the gap: a critical step forward towards the design and discovery of potential drugs, Journal Biologia 72 (2017) 1-13.

[14]. M. Balmith, M. Faya, M.E. S. Soliman, Ebola virus: A gap in drug design and discovery - experimental and computational perspective,

Chemical Biology and Drug Design 89 (2017) 297–308.
[15]. B. Hartlieb, T. Muziol, W. Weissenhorn, S. Becker, Crystal structure of the C-terminal domain of Ebola virus VP30 reveals a role in transcription and nucleocapsid association, Proceeding of National Academy of Science, USA 104 (2007) 624-629.
[16]. Y. Guo, S.S. Dong, P. Yang, G.B. Li, B.C. Liu, C. Yang, Z.H. Rao, Crystal structure of Ebola virus nucleoprotein core domain at 1.8A resolution, Protein Cell 6 (2015) 351-362.
[17]. R.N. Kirchdoerfer, C.L. Moyer, D.M. Abelson, E.O. Saphire, Ebola virus VP30 CTD bound to 8-nucleoprotein PLoS Pathog 12 (2016) e1005937.
[18]. Spartan user's guide, Wave function, Inc, Irvine, CA 92612 USA
[19]. W.J. Hehre, L. Radom, P.V.R. Schleyer, J.A. Pope, Ab initio molecular Orbital Theory, Wiley, New York, 1988.
[20]. A.D. Becke, Density-functional thermochemistry. III. The role of exact exchange, Journal Chemical Physics 98 (1993) 5648. DOI: 10.1063/1.464913
[21]. C. Lee, W. Yang, R.G. Parr, Development of the Colle-Salvetti correlation-energy formula into a functional of the electron density, Physical Review B 37 (1988) 785-789. DOI: 10.1103/physrevb.37.785
[22]. Spartan'14 Wavefunction, Inc. Irvine, CA, 2014
[23]. M.N. Wass, L.A. Kelley, M.J.E. Sternberg, 3DLigandSite: predicting ligand-binding sites using similar structures, Nucleic Acids Research 38 (2010) W469–W473.
[24]. O. Trott, A.J. Olson, AutoDockVina: improving the speed and accuracy of docking with a new scoring function, efficient optimization and multithreading, Journal of Computational Chemistry 31 (2010) 455–461.
[25]. A.K Oyebamiji, E.K. Oladipo, T.M. Olotu, H.E. Awoyelu, E. Adamolekun, B. Semire, In-vitro Investigation on Selected compounds in Annona Muricata Seed: A Potential SARS-CoV nsp12 Polymerase Inhibitors down Regulating 2019-nCoV, International Journal of Traditional Natural Medicine 10 (2020) 13-23.
[26]. A.K. Oyebamiji, G.F. Tolufashe, B. Semire, Inhibition study on anti-type 3 of 3α-hydroxysteroid dehydrogenase activity against 1,2,3-triazolo[4,5-D]pyrimidine derivatives: Molecular modelling approach, Scientific African 8 (2020) e00444.
[27]. A.K. Oyebamiji, O.A Fadare, B. Semire, Hybrid-based drug design of 1,2,3-triazolepyrimidine-hybrid derivatives: Efficient inhibiting agents of mesenchymal–epithelial transition factor reducing gastric cancer cell growth, Journal of Chemical Research 44 (2020) 277-280. DOI: 10.1177/1747519819898354
[28]. R.O. Oyewole, A.K. Oyebamiji, B. Semire, Theoretical Calculations of Molecular Descriptors for Anticancer Activities of 1,2,3-Triazole-pyrimidine derivatives against Gastric cancer cell (MGC-803): DFT, QSAR and Docking Approaches, Heliyon 6 (2020) e03926. DOI: 10.1016/j.heliyon.2020.e03926
[29]. A.E. Adegbola, O.S. Fadahunsi, A.A. Ayodeji Z. Abijo, T.A. Balogun, T.S. Aderibigbe, B. Semire, P.I. Adegbola, Computational prediction of nimbanal as potential antagonist of respiratory syndrome coronavirus, Informatics in Medicine Unlocked 24 (2021) 100617. DOI: 10.1016/j.imu.2021.100617
[30]. P.I. Adegbola, O.S. Fadahunsi, A.E. Adegbola, B. Semire, In silico studies of potency and safety assessment of selected trial drugs for the treatment of COVID-19, In Silico Pharmacology 9 (2001) 45. DOI: 10.1007/s40203-021-00105-x
[31]. P.I. Adegbola, B. Semire, O.S. Fadahunsi A.E. Adegoke, Molecular docking and ADMET studies of *Allium cepa*, *Azadirachta indica* and *Xylopia aethiopica* isolates as potential anti-viral drugs for Covid-19, Virus Disease 32 (2021) 85-97.
[32]. A.K. Oyebamiji, S.A. Akintelu, O.P. Amao, M.O. Kaka, A.E. Morakinyo, F.A. Amao, B. Semire**,** Dataset on theoretical bio-evaluation of 1,2,4-thiadiazole-1,2,4-triazole Analogues against epidermal growth factor receptor kinase down regulating human lung cancer. Data in Brief. 37 (2021) 107234. DOI: 10.1016/j.dib.2021.107234
[33]. M.A.F. Nasution, E.P. Toepak, A.H. Alkaff, U.S. Tambunan, Flexible docking-based molecular dynamics simulation of natural product compounds and Ebola virus Nucleocapsid (EBOV NP): a computational approach to discover new drug for combating Ebola, BMC Bioinformatics 19 (2018) 419. DOI: 10.1186/s12859-018-2387-8
[34]. Y. Antonius, J. Ongko, J. Sukweenadhi, S.E. Dwi Putra, Identification of potential Ebola virus nucleoprotein (EBOV NP) inhibitor derivate from various traditional medicinal plants in Indonesia: *in silico* study, Media Pharmaceutica Indonesiana 3 (2021) 217-226.
[35]. R.N. Kirchdoerfer, C.L. Moyer, D.M. Abelson, E.O. Saphire, The Ebola Virus VP30-NP Interaction Is a Regulator of Viral RNA Synthesis. PLoS Pathog 12 (2016) e1005937. DOI: 10.1371/journal.ppat.1005937
[36]. F. Darvas, G. Keseru, A. Papp, G. Dorman, L. Urge, P. Krajcsi, In Silico and Ex silico ADME approaches for drug discovery, Topics in Medicinal Chemistry 2 (2002) 1287–304.
[37]. H. Wen, H. Jung, X. Li, Drug delivery approaches in addressing clinical pharmacology-related issues: Opportunities and challenges, AAPS Journal 17 (2015) 1327–1340.
[38]. C.A. Lipinski, Lead- and drug-like compounds: the rule-of-five revolution, Drug Discovery Today: Technologies 1 (2004) 337-341. DOI: 10.1016/j.ddtec.2004.11.007
[39]. A. Daina, V. Zoete, ABOILED-Egg to predict gastrointestinal absorption and brain penetration of small molecules, ChemMedChem 11 (2016) 1117–1121.
[40]. S.A. Attique, M. Hassan, M. Usman, R.M. Atif, S. Mahboob, K.A. Al-Ghanim, M. Bilal, M.Z. Nawaz, A molecular docking approach to evaluate

the pharmacological properties of natural and synthetic treatment candidates for use against hypertension, International Journal of Environmental Research and Public Health 16 (2019) 923. DOI: 10.3390/ijerph16060923

[41]. D.E.V. Pires, T.L. Blundell, D.B. Ascher, pkCSM: predicting small-molecule pharmacokinetic and toxicity properties using graph-based signatures, Journal of Medicinal Chemistry 58 (2015) 4066–4072.

[42]. M.J. Waring, J. Arrowsmith, A.R. Leach, P.D. Leeson, S. Mandrell, R.M. Owen, An analysis of the attrition of drug candidates from four major pharmaceutical companies, Natural Review of Drug Discovery 14 (2015) 475–486.

[43]. D.A. Flockhart, Drug Interactions: cytochrome P450 Drug Interaction Table. Indiana University School of Medicine'/clinpharm/ddis/clinical-table/''. 2007; Accessed August 12th 2018

Received: 02.09.2021
Received in revised form: 01.03.2022
Accepted: 03.03.2022